Morphological operators on the unit circle

A. G. Hanbury and J. Serra*

May 2001

Abstract

Images encoding angular information are common in image analysis. Examples are the hue band of colour images, or images encoding directional texture information. Applying mathematical morphology to image data distributed on the unit circle is not immediately possible, as the unit circle is not a lattice. Three approaches to this problem are presented. Firstly, difference based operators are studied (e.g. gradient, top-hat). Secondly, a definition of grouped circular data is suggested, and "pseudo" morphological operators, which operate only on grouped data are introduced. Lastly, the treatment of these images as labelled images is presented, leading to the development of a cyclic opening operator. Applications to treating the hue band of colour images and to finding perturbations in wood texture are given.

1 Introduction

In image analysis, one often has to treat data distributed on the unit circle. The two studies which motivated the development of the theoretical elements presented in this article illustrate some situations encountered often: The first involves the description of directional textures, and the other, the filtration of the hue component in colour images.

*Both authors are with the Centre de Morphologie Mathématique, Ecole des Mines de Paris, 35 rue Saint-Honoré, 77300 Fontainebleau, France. E-mail should be sent to: Hanbury@cmm.ensmp.fr

The application of morphological operators to the hue band of colour images is related to another subject which has received much attention, morphology for vector images, specifically colour images. A number of possible orders for colour vectors in the RGB colour space have been proposed [1] [2] [4] [9]. Work using an angular representation of hue, and hence more closely related to the approach presented in this article is presented by Peters [5], who develops morphological operators on the hue circle which require the choice of an origin; Demarty and Beucher [3] who treat image segmentation in the HLS colour space; and Zhang and Wang [11] who present definitions of two distances on the hue circle in the context of colour image segmentation.

The unit circle, like the round table of King Arthur's knights, has no order of importance, and no dominant position. In mathematical terms, this signifies that we cannot construct a lattice on the unit circle, unless assigning it an arbitrary origin. This is a severe verdict against morphological treatments (i.e. operators relying on lattices) when we use them on the unit circle.

However, is it really impossible to bypass this interdiction? If we consider the standard morphological operators, three paths seem possible. Firstly, there is the class of operators which bring into play a difference, such as gradients, top-hats, medians, etc. Does this difference not introduce a local origin, obviously variable at each point, but sufficient to transfer to the circular case? Section 2 treats these operators.

The second approach, covered in section 3, considers the grouping of circular data. Deciding on the number of groups in a dataset is not straightforward, so we introduce a simple criterion for grouped data, and define the basic morphological operators so that they act only if a structuring element contains grouped data.

The third approach, developed in section 4, involves a different way of viewing the situation. A sequence of labels with index $i \in$ defined on the unit circle can serve to index the angles. There could be a royal blue class, an apple green class, etc., with the condition that the labels with numbers $i+N$ are identical to those numbered i. If every pixel in the image is assigned a label, then we have an indexed partition of the image. With two labels, one is in a situation analogous to that of a binary image. For this case, the alternating filters of type $\varphi\gamma$ (i.e. the result of a composition of an opening by a closing) can also be viewed as the product of two openings operating successively on the two labelled regions "foreground" and "background". If, instead of two labels, we have N, and if we perform a cycle of N openings

(a)

(b)

Figure 1: The images used in the examples

successively on each of the labelled regions, what is the result?

2 Circular centered operators

We fix an origin a_0 on the unit circle C with centre o by, for example, choosing the topmost point, and indicate the points a_i on the circle by their curvilinear coordinate in the trigonometric sense between 0 and 2π from a_0. Given two points a and a', we use the notation $a \div a'$ to indicate the value of the acute angle aoa', i.e.

$$a \div a' = \begin{cases} |a - a'| & \text{if} \quad |a - a'| \leq \pi \\ 2\pi - |a - a'| & \text{if} \quad |a - a'| \geq \pi \end{cases} \tag{1}$$

If the a_i are digital values between 0 and 255 (for example), the expression "$\leq \pi$" becomes "≤ 127", and "2π" becomes "255". However, we continue using the notation in terms of π, as it is more enlightening.

Relation 1 appears in [5] applied to the treatment of the hue band of colour images. We use it here to provide a complete ordering of the points on the circle C using the following algorithm:

$$a_i \succeq a_j \begin{cases} \text{if} & a_i \div a_0 \geq a_j \div a_0 \\ \text{or if} & a_i \div a_0 = a_j \div a_0 \text{ and } a_i - a_0 \leq \pi \end{cases}$$

2.1 Gradient

We know that in the Euclidean space ^{d}, to determine the modulus of the gradient, at point x, of a numerical differentiable function f, one considers a small sphere $S(x, r)$ centered on x with radius r. Then one takes the supremum minus the infimum of the increments $|f(x) - f(y)|$, where y describes the small sphere $S(x, r)$, i.e.

$$2g(x, r) = \vee \{|f(x) - f(y)|, y \in S(x, r)\} - \wedge \{|f(x) - f(y)|, y \in S(x, r)\} \tag{2}$$

Finally, one determines the limit of the function $g(x, r)$ as r tends to zero. This limit exists as the function f is differentiable in x. In the two-dimensional digital case, it is sufficient to apply relation 2, taking for $S(x, r)$ the unit circle centered on x (square or hexagon). This is the classic Beucher algorithm [7] for the gradient.

Consider now an image of hues or of directions, i.e. a function $a : E \to C$, where E is an Euclidean or digital space, and C is the unit circle. As the previous development only involves increments, we can transpose relation 2 to the circular function a by replacing all the $|a(x) - a(y)|$ by $|a(x) \div a(y)|$. This transposition then defines the modulus of the gradient of the circular distribution. For example, in ^{d}, $K(x)$ indicates the set of neighbours at distance one from point x, hence

$$(\text{grad} : \text{a})(x) = \frac{1}{2} \vee \{|a(x) \div a(y)|, y \in K(x)\} - \frac{1}{2} \wedge \{|a(x) \div a(y)|, y \in K(x)\} \tag{3}$$

As an illustration, consider the hue component of figure 1a, shown in figure 2a. This image was chosen as it is mostly red in colour, and in the angular hue encoding, red usually usually has hue values around 0°. This means that pixels which appear red could have low hue values (for example, 0° to 30°) and high hue values (330° to 360°). A large discontinuity is therefore visible in the hue image, with red pixels appearing at the extremities of the histogram (figure 2b). A classical gradient on this hue band produces a large number of spurious high-valued pixels, as shown in figure 2c.

These high-values are present even though the neighbouring pixels appear very similar in colour, and are due to the discontinuity in the hue encoding. A good illustration of this is the outer part of the halo, which appears smooth in figure 1a, but results in very high gradients in figure 2c. The gradient calculated using equation 3, shown in figure 2d, overcomes this problem. Note that if we rotate the hue band pixel values by π, the classical gradient will be the same as the angular gradient. The angular gradient is, however, invariant to rotations of the pixel values.

2.2 Top-hat

The notion of the "top-hat", in the sense of F. Meyer [7], is the residue between a numerical function and its transformation by an opening. It therefore only involves increments, and hence can be transposed to functions of values in C. We explain below the algorithm for the use of openings by adjunction (i.e. products by composition of an erosion by the adjunct dilation). We begin by reminding the reader of the relation which gives the value $\gamma_B(x)$ of the opening by the structuring element B, at point x. If we indicate by

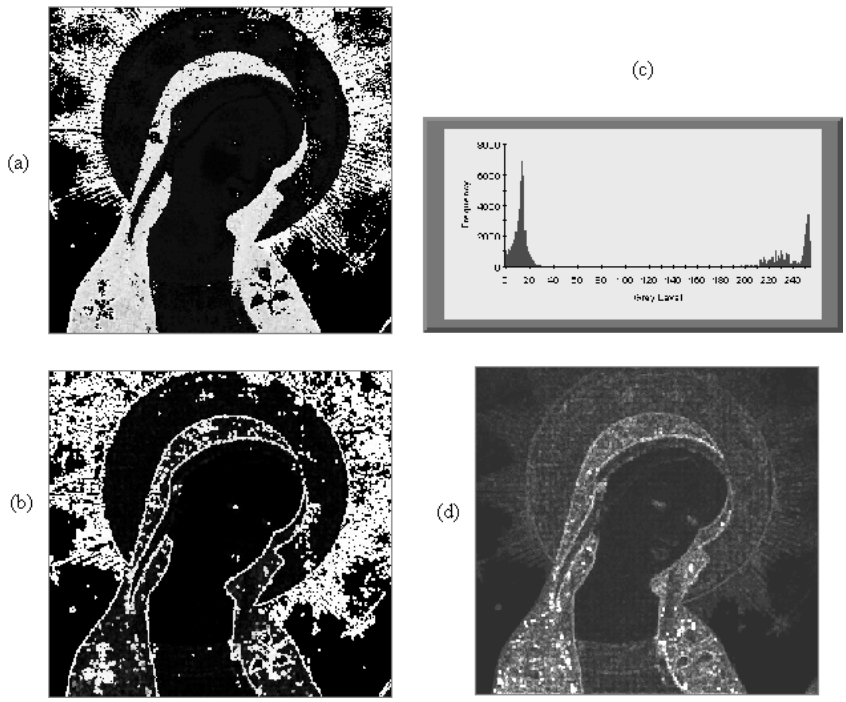

Figure 2: a: The hue band of the virgin image (figure 1); b: The histogram of the hue band; c: The classical gradient on the hue band; d: The angular gradient on the hue band.

$\{B_i, i \in I\}$ the family of structuring elements which contain point x

$$\gamma_B(x) = \sup\{\inf[f(y), y \in B_i], i \in I\}$$

For the top-hat $f(x) - \gamma_B(x)$ we therefore write

$$f(x) - \gamma_B(x) = -\sup\{\inf[f(y) - f(x), y \in B_i], i \in I\} \quad (4)$$

in which there are only increments of the function f around point x. We can therefore transpose to functions of circular values a exactly as we did for the gradient, and give the definition

$$(\text{top} - \text{hat})(x) = -\sup\{\inf[-(a(x) \div a(y)), y \in B_i], i \in I\} \quad (5)$$

An example of a top-hat of this type is given in figure 3. Figure 3a is a subsection of the luminance band of figure 1b which contains some regions (indicated by the white rectangles) in which the dominant colour is red, that is, they fall on the hue discontinuity, as is seen in the corresponding regions in the hue image, figure 3b. A classical white top-hat (equation 4) applied to the hue band is shown in figure 3c, with its histogram in figure 3e.

Once again, it is evident that even though there is not much visible change in the colour within the indicated regions, they result in very noisy top-hats. This is further demonstrated by the relatively large number of pixels near the upper end (360°) of the histogram. The result of applying the circular centred top-hat (equation 5) is shown in figure 3d, with its histogram in figure 3f. In this image, the spurious high-valued pixels do not appear.

An alternative definition of the top-hat is given in section 4.

3 Pseudo operators

The main shortcoming of the unit circle morphological operators proposed in [5] is the requirement to choose an origin, which in some cases would lead to the user having to make an arbitrary choice. In this section, we propose an alternative formulation, where one is not required to choose an origin, but instead must provide a definition of grouped circular data. We introduce a possible definition of grouped data in the framework of the morphological centre, and then extend this definition to the erosion and dilation operators.

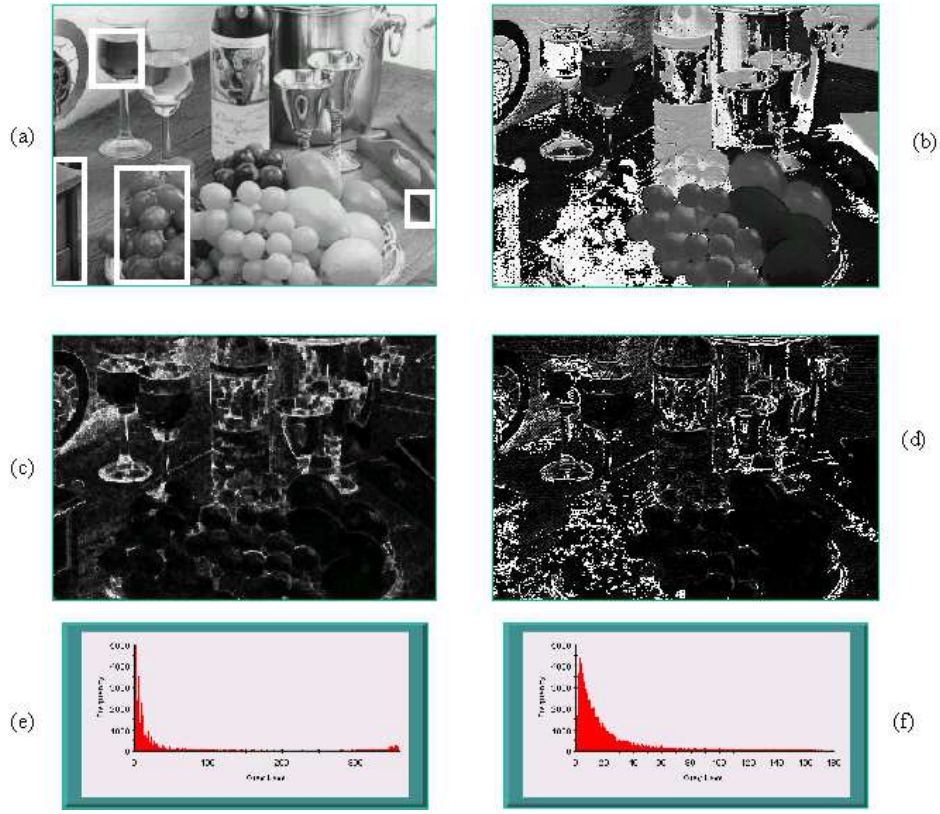

Figure 3: a: A subsection of fig1b with the red parts marked (image size 311 x 227 pixels); b: The hue band of image a; c: The classic white top-hat with a 3x3 square of image a; d: The circular centred top-hat with a 3x3 square of image a; e: The histogram of image c; f: The histogram of image d.

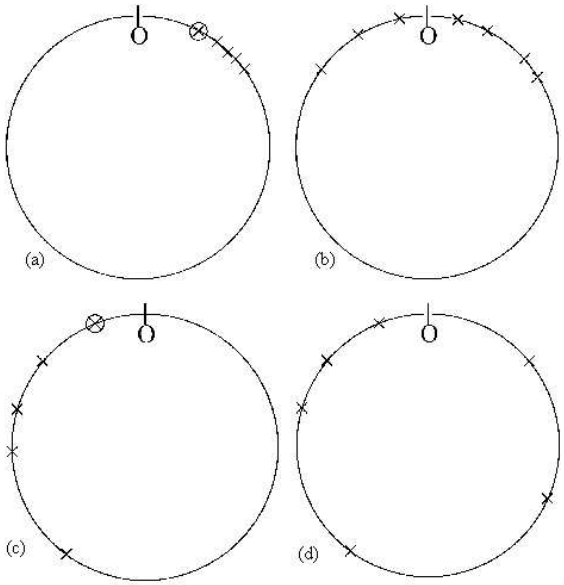

Figure 4: Four distributions of circular data, a , b and c are ω-grouped, d is not.

3.1 Morphological centre

The morphological centre is a notion which naturally appears in the self-dual morphological filters [8]. Consider n numerical values $t_i \in R$ and a number t which we wish to bring closer to the t_i. The "Morphological Centre" operator κ acts as follows

$$\kappa(t) = \begin{cases} \wedge t_i & \text{if} \quad t \leq \wedge t_i \\ t & \text{if} \quad \wedge t_i \leq t \leq \vee t_i \\ \vee t_i & \text{if} \quad \vee t_i \leq t \end{cases} \tag{6}$$

In particular, for $n = 2$ we find the median between three values t_1, t_2 and t. The identification can be expanded by iteration to $n > 2$. We, however, limit ourselves to transposing algorithm 6 to circular data.

A difficulty is, however, apparent. On the line, we can always say whether a value t is exterior (superior or inferior) to t_i. On the circle, we can make sense of this expression in the case of distributions such as those in figure 4a, b and c, but not in figure 4d, where the data is too dispersed. We describe two approaches:

1. We replace a unconditionally by the closest a_i, by applying

$$\kappa_0(a) = \{a_i \,|(a_i \div a) = \wedge(a_i \div a), i \in I\}$$

2. Alternatively, we construct conditions similar to those in relation 6. It therefore becomes necessary to formally define the notion of a group of points, of which figures 4a–c give an intuitive idea.

Definition: We say that a family $\{a_i, i \in I\}$ of points on a unit circle are ω-grouped when there exists an origin such that

$$(\vee a_i, i \in I) - (\wedge a_i, i \in I) \leq \omega \leq \pi \tag{7}$$

where ω is an angle less then or equal to π.

The condition $\omega \leq \pi$ suppresses the case shown in figure 4d. The following proposition characterises the groups of points using their coordinates.

Proposition: The family $\{a_i, i \in I\}$ of the points on the unit circle C forms an ω-group if and only if one has

$$\vee\{a_i, i \in I\} - \wedge\{a_i, i \in I\} \leq \omega \tag{8}$$

for an arbitrary origin a_0, or for the origin $a_0 + \pi$.

Proof: If the a_i are ω-grouped, there exists a partition of C into two semi-circles so that all the a_i are found in one of the semi-circles. If we take for a_0 some point in the opposite semi-circle, the relation 8 is verified, because a_0 does not belong to the envelope of the group of points (i.e. to the smallest sector of the circle which contains them all). Conversely, if the relation 8 is satisfied for an origin a_0, it is sufficient to move this origin to the point $\wedge\{a_i, i \in I\}$ to get relation 7, the definition of an ω-group of the a_i.

The algorithm defining the circular morphological centre develops directly from the preceding proposition. It is sufficient to take as the origin the point a that we wish to compare to the family $\{a_i\}$. We simply remember that, as we must use positive coordinates, the differences implicit in a change of origin are written thus

$$\text{dif}(a_i, a) = \begin{cases} a_i - a & \text{if} \quad a_i - a \geq 0 \\ 2\pi + a_i - a & \text{otherwise} \end{cases}$$

Definition: Given a family $\{a_i, i \in I\}$ and a point on the unit circle, and hence a grouping angle ω, the transformation $\kappa(a)$ of a by morphological centering is defined as

$$\kappa(a) = \begin{cases} a & \text{if} \quad \alpha \geq \pi \\ \wedge a_i & \text{if} \quad \alpha \leq \pi \text{ and } (a \div \wedge \{a_i, i \in I\}) < (a \div \vee \{a_i, i \in I\}) \\ \vee a_i & \text{if} \quad \alpha \leq \pi \text{ and } (a \div \vee \{a_i, i \in I\}) < (a \div \wedge \{a_i, i \in I\}) \end{cases}$$

with $\alpha = \vee \{\text{dif}(a, a_i), i \in I\} - \wedge \{\text{dif}(a, a_i), i \in I\}$.

In other words, if there is an ω-group and a is outside the group ($\alpha \leq \pi$), one replaces a by the extremity of the group closest to a. If there is no grouping, or if a is inside the ω-group of the a_i ($\alpha \geq \pi$ for both these cases), one leaves it unchanged. In the case of figure 4, if we take the origin as the point to transform, it does not change for figures 4b and d, and becomes the circled point in figures 4a and c. In [10], a similar subject, the colour median filter operating on three-dimensional colour vectors in RGB space, is treated.

3.2 Erosion and dilation

The notion of an ω-group (relation 7) suggests the introduction of two operators which approximate a supremum and an infimum. Consider a finite ω-group $\{a_i, i \in I\}$. For all the origins for which relation 8 is valid, the number $a_{\max} = \vee \{a_i, i \in I\}$, even though variable as a function of the origin, always corresponds to the same point of the group. The same applies to the infimum $\wedge \{a_i, i \in I\}$. These two extremities therefore have a significance partially independent of the choice of the origin on the unit circle.

This observation leads naturally to the introduction of a "pseudo-dilation" operator. Consider a function $a : E \to C$, i.e. for every point x in the space E, $a(x)$ is a value on the unit circle, and let $B(x)$ be a structuring element, i.e. an arbitrary function $B : E \to \mathcal{P}(E)$. The pseudo-dilation $\delta : C^E \to C^E$ is defined as

$$(\delta(a))(x) = \begin{cases} \vee \{a_i(y), y \in B(x)\} & \text{if} \quad \{a_i(y), y \in B(x)\} \text{ forms a } \pi-\text{group} \\ a(x) & \text{otherwise} \end{cases}$$

The operator δ certainly depends on the choice of the origin but, by construction, commutes with the rotations on the unit circle (i.e. with changes of the origin). It is not a dilation, as one cannot find an underlying order

relation, and not, a fortiori, a lattice. Nevertheless, for all symmetric B we can define, by duality, a "pseudo-erosion"

$$(\epsilon(a))(x) = \begin{cases} \wedge\{a_i(y), y \in B(x)\} & \text{if} \quad \{a_i(y), y \in B(x)\} \text{ forms a } \pi-\text{group} \\ a(x) & \text{otherwise} \end{cases}$$

It follows that all the classic extensive operators in mathematical morphology, such as openings, closings, reconstruction, levelling, etc., have a "pseudo" version.

Figure 5 provides a comparison between the pseudo-erosion and standard erosion. Figure 5a is the hue band of a subsection of figure 1b. Figure 5b shows a pseudo-erosion and figure 5c, a standard erosion of this hue band. The region in which the differences are most pronounced is for the red fruit to the left of the image. The hue values for red straddle the discontinuity at $0°/360°$, and the standard erosion reduces these to small values greater than zero. The pseudo-erosion, however, replaces the pixels with the infimum of the group of values around $0°$. One should notice the regions, such as the base of the wine glass, where this erosion operator does not change the pixel values as they do not form an ω-group.

In introducing these pseudo operators to avoid the necessity of choosing an origin, one unfortunately loses a number of desirable properties of standard morphological operators. One example is that the pseudo-opening and pseudo-closing operators are not idempotent (but are usually idempotent after a few iterations). This lack of idempotence is due to the pseudo-operators not acting in the same way on all pixels, but leaving some pixels in their original states. The decision as to whether to leave a pixel or change it depends on the distribution of the values of the pixels in the structuring element, and this distribution changes after each application of an operator.

4 Labelled openings

Circular data may be treated in another manner, which is more set oriented, and where there is no obligation to define groups or work on increments. This third approach is based on the idea of first labelling the points of the working space according to the local hue or angle, then processing the obtained sets, and finally combining the results in an isotropic way.

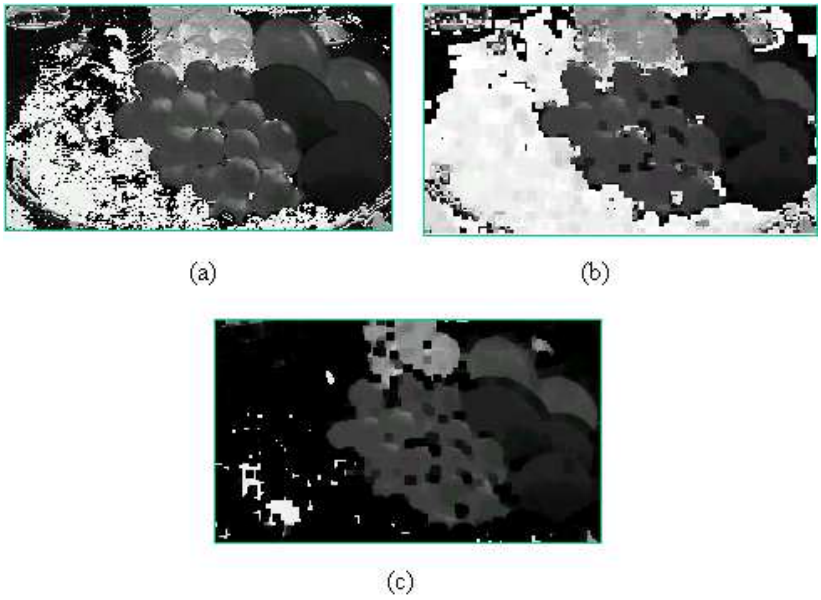

Figure 5: a: The hue band of a subsection of figure 1a (image size 231x134 pixels); b: A pseudo-erosion of image a; c: A standard erosion of image a. Both erosions are 5x5 pixel square

4.1 Theory

Denote by $A(\alpha,\omega)$ the set of those points $x \in E$ whose angular value $a(x)$ lies in acute sector $[\alpha, \alpha+\omega]$

$$A(\alpha,\omega) = \{x : x \in E, a(x) \in [\alpha, \alpha+\omega]\}$$

Now let $\{\gamma_\lambda, \lambda > 0\}$ be an opening of size λ on $\mathcal{P}(E)$. The opening $\gamma_\lambda A(\alpha,\omega)$ is performed as for a binary opening, with $A(\alpha,\omega)$ treated as the foreground, and the rest as the background. In order to isotropise this operation, we take the union of all transforms $\gamma_\lambda[A(\alpha,\omega)]$ as α traces out the unit circle, i.e.

$$\underline{\gamma}(\lambda,\omega) = \bigcup \{\gamma_\lambda[A(\alpha,\omega)], 0 \le \alpha \le 2\pi\} \tag{9}$$

The result is a binary image containing as foreground all the pixels which are not removed by the action of the opening for one of the angles α. The residue (in the sense of the top-hat) of this opening is obtained by inverting $\underline{\gamma}(\lambda,\omega)$, that is,

$$\underline{R}_\gamma(\lambda,\omega) = \overline{\underline{\gamma}(\lambda,\omega)} \tag{10}$$

The residue consists of the pixels which were eliminated by the opening for all angles α.

When the angle ω varies from 0 to π, it is clear that the opening $\underline{\gamma}$ is an increasing function of ω. As usual, this opening is also a decreasing function of the size parameter λ. These considerations lead to the following proposition:

Proposition: Let $a : E \to C$ be a function of circular values, γ_λ a granulometry on $\mathcal{P}(E)$, and $A(\alpha,\omega) : \mathcal{P}(E) \to \mathcal{P}(E)$ the angular restriction

$$A(\alpha,\omega) = \{x : x \in E, a(x) \in [\alpha, \alpha+\omega]\}$$

Then the operator

$$\underline{\gamma}(\lambda,\omega) = \bigcup \{\gamma_\lambda[A(\alpha,\omega)], 0 \le \alpha \le 2\pi\}$$

is an isotropic opening. The family $\left\{\underline{\gamma}(\lambda,\pi-\omega), 0 \le \omega \le \pi, \lambda > 0\right\}$ engenders a *double granulometry* with respect to the two parameters λ and $\pi - \omega$.

The above labelled openings treat the data in a parallel way (each $\gamma_\lambda[A(\alpha,\omega)]$ could be performed by an independent processor, for example).

4.2 Application

An industrial application of the labelled opening is presented. When sorting oak boards destined to be used to make furniture, it is necessary to find the knots, and to measure the sizes of the small light patches. These two characteristics have been highlighted in figure 6a, where the knots are surrounded by black rectangles and the light patches by white rectangles (the three light horizontal lines in this image are chalk lines drawn on the board). Knots can be found using colour and texture characteristics, as they are usually much darker than the surrounding wood, and usually perturb the directions of the surrounding grain lines. The light patches are generally of a similar colour to other parts of the wood, but tend to cut grain lines, causing a disruption in the dominant local texture orientation. An application of the labelled opening operator to finding regions of anomalous texture orientation is presented here.

Wood texture is oriented, meaning that there is a dominant direction in the neighbourhood of each image point. This texture can therefore be represented by an image encoding the dominant orientation in each pixel neighbourhood. An algorithm based on that developed by Rao [6] is used to extract these orientations. The steps in this algorithm are:

1. Detection of the edges of the wood and cropping of the image to contain only the wood.

2. Convolution by a Gaussian filter of size 5×5.

3. Calculation of the angle at every pixel in the image from the horizontal and vertical gradients.

4. Determination of the dominant angle within a moving frame of size 16×16 pixels, moved in steps of 8 pixels horizontally and vertically.

5. Construction of the reduced size orientation image which encodes the dominant orientation in each frame by a single pixel.

As the orientation of a grain line can equally well be described by two directions, namely θ and $\theta+180°$, the angles have values between $0°$ and $180°$, such that $\theta + 180° = \theta$. The reduced size orientation image for figure 6a is shown in figure 6c.

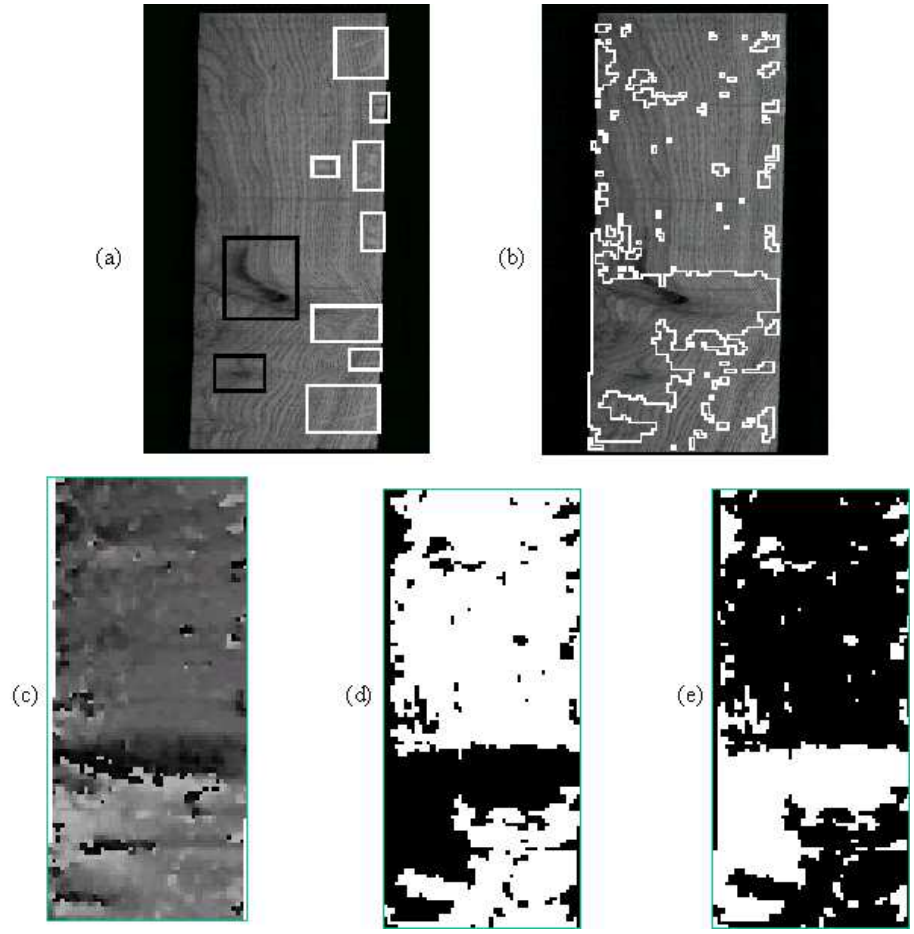

Figure 6: a: an oak board with knots (indicated by black rectangles) and light patches (indicated by white rectangles) (image size 608x955 pixels); b: The residue of the labelled opening on the orientation image expendd and projected onto the original image (the regions enclosed by the white outlines correspond to the residue); c: The reduced orientation image (size 50x112 pixels) calculated using the Rao algorithm; d: The union of the opening of each labelled region; e: The residue of the labelled opening on the orientation image

The aim is for the regions of anomalous orientation to appear as the residue of a labelled opening. We used a connected labelled opening (opening with reconstruction) with $\omega = 45°$ and a square structuring element with side of length 9 pixels. The isotropisation of the opening (equation 9) was approximated by varying α from $0°$ to $157.5°$ in steps of $22.5°$. The resulting label definitions are shown in figures 7b and 7d, and the corresponding labelled images in figures 7a and 7c (two labelled images are shown as the angular values of the labels overlap). The numbers shown on the label definition diagrams indicate the order of the labelling as the value of α increases. The result of the opening on each of the labels in 7a and 7c are shown respectively in 7e and 7f, where the lightest grey represents the regions eliminated by the opening operator. The union of the labelled regions not eliminated by the opening (equation 10) is shown in figure 6d. The residue (the inverse of figure 6d) is shown in figure 6e, and this residue expanded and projected onto the original image is shown in figure 6b, where the regions enclosed by the white outlines correspond to the residue.

The region of severe perturbation of grain lines due to the knots on the lower part of the wood is found, although the upper part of the largest knot is not detected as it is parallel to the grain lines forming the largely homogeneous upper region of the board. Most of the light patches are also detected. There are afew false detections, corresponding to regions where there is a change in the direction of the grain lines without an associated defect (for example, at the top left of board), or to tiny misdetections which could be eliminated by a subsequent area opening.

This algorithm has been applied to an algorithm of 60 oak images with good results. However, even though defects are associated with texture orientation perturbations, the presence of such a perturbation does not guarantee the presence of a defect. The results of this transform should therefore ideally be used as input to a decision procedure, which uses colour and further texture information to calculate the likelihood of a defect being present.

5 Conclusion

Three possible approaches to applying mathematical morphology to angular data have been presented. The first involves using differences (increments), the second makes use of a definition for grouped circular data, and the third

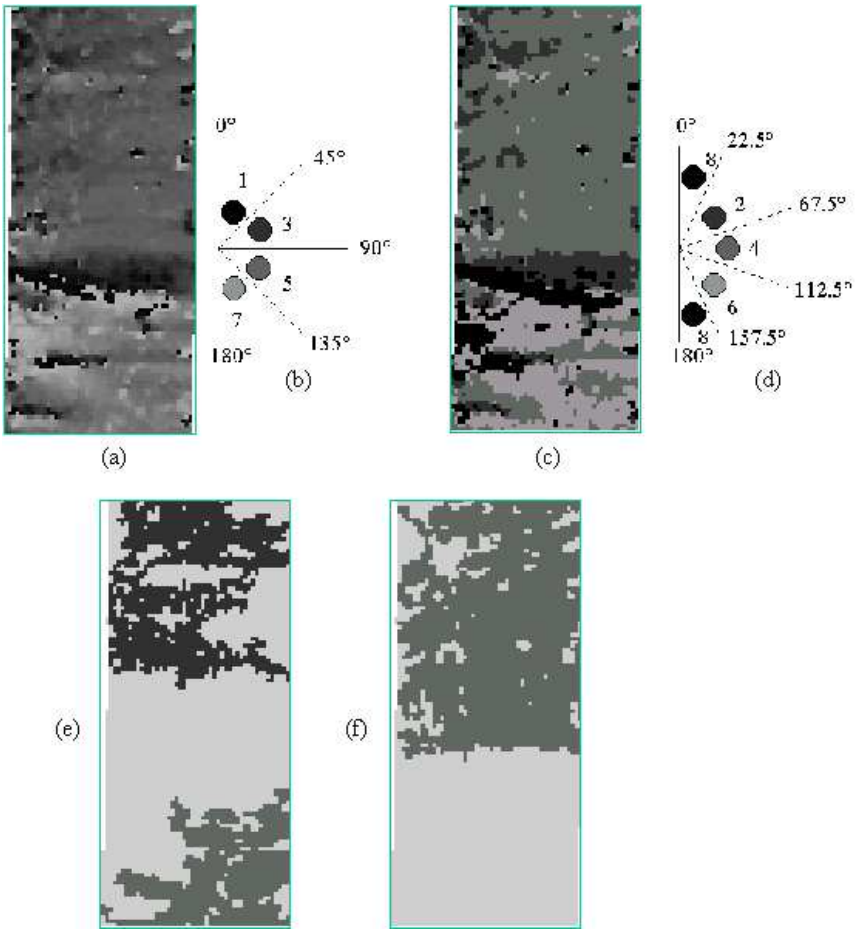

Figure 7: a and c: The labels defined on the orientation image (figure 6c); b and d: The labelled definitions; e: The opening by a square of side 9 pixels of each label shown in image a (the lightest grey represents the labelled regions eliminated by the opening); f: The same opening performed on image c.

uses labels. Difference versions of the gradient and top-hat are presented. Secondly, a formulation of "pseudo" versions of the erosion and dilation operators are given, which can be expanded to create the other standard morphological operators. They have the advantage of not requiring the choice of an origin on the circle, but unfortunately suffer from some unfortunate properties such as the non-idempotence of the pseudo-opening and pseudo-closing operators. Lastly, openings on labelled images are presented. Applications of these operators to the hue band of colour images and to images encoding angular texture information are given. In practical applications, we find that the use, if possible, of the circular-centred operators or labelled operators give the best results.

The reader should be aware that in most cases, angular data does not appear alone, but is combined with other non-circular values. For colour images, these are usually luminance or intensity and saturation; and for oriented textures, measures of magnitude or coherence. More generally, the question arises with vector data, when one wants their processing to be independent of the choice of the vector base. For example, a 2-D Euclidean vector (x, y) may be represented in polar coordinates (ρ, θ). Then any processing that combines the above circular operators (for θ) with operators on ρ yields a result that does not depend on the orientation of the initial base (x, y). A similar comment applies in ^{3} when vectors are decomposed into their spherical or their cylindrical representations. The development of operators which treat these non-angular values along with the related angular quantities in a rotationally invariant way is an interesting topic for further development.

Finally, we note that a detailed experimental comparison of the angular morphological operators with standard operators on the same data set is not done, as it is immediately obvious from the data which approach should be used. If, during the analysis of a set of data or an image, one has to choose an arbitrary origin before applying an operator, then the rotationally invariant operators in this article are to be preferred.

References

[1] J. Chanussot and P. Lambert. Total ordering based on space filling curves for multi-valued morphology. In *Proceedings of the International Symposium on Mathematical Morphology (ISMM '98)*, pages 51-58, 1998.

[2] Mary L. Comer and Edward J. Delp. Morphological operations for color image processing. *Journal of Electronic Imaging*, 8(3):279-289, July 1999.

[3] Claire-Hélène Demarty and Serge Beucher. Color segmentation algorithm using an HLS transformation. In *Proceedings of the International Symposium on Mathematical Morphology (ISMM '98)*, pages 231-238, 1998.

[4] M.C. d'Ornellas, R. Boomgaard, and J. Geusebroek. Morpholocal algorithms for color images based on a generic-programming approach. In *Proceedings of the XI Brazilian Symposium on Computer Graphics and Image Processing (SIBGRAPI'98*). IEEE Press, 1998.

[5] R. A. Peters II. Mathematical morphology for angle-valued images. In *Non-Linear Image Processing VIII.* SPIE volume 3026, 1997.

[6] A. R. Rao. *A taxonomy for texture description and identification.* Springer-Verlag, 1990.

[7] J. Serra. *Image Analysis and Mathematical Morphology.* Academic Press, London, 1982.

[8] J. Serra. *Image Analysis and Mathematical Morphology Volume 2 : Theoretical Advances.* Academic Press, London, 1988.

[9] H. Talbot, C. Evans and R. Jones. Complete ordering and multivariate mathematical morphology: Algorithms and applications. In *Proceedings of the International Symposium on Mathematical Morphology (ISMM '98)*, pages 27-34, 1998.

[10] P. E. Trahanias, D. Karakos, and A.N. Venetsanopoulos. Directional processing of color images: Theory and experimental results. *IEEE Transactions on Image Processing*, 5(6):868-880, June 1996.

[11] Chi Zhang and P. Wang. A new method of color image segmentation based on intensity and hue clustering. In *Proceedings of the 15th ICPR, Barcelona*, volume 3, pages 617-620, 2000.